Synthesis and Characterization of Six New Quaternary Actinide Thiophosphate Compounds: $Cs_8U_5(P_3S_{10})_2(PS_4)_6$, $K_{10}Th_3(P_2S_7)_4(PS_4)_2$, and $A_5An(PS_4)_3$, (A = K, Rb, Cs; An = U, Th)

Ryan F. Hess,[†,#] Kent D. Abney,[#] Jennifer L. Burris,[‡] H. Dieter Hochheimer,[‡] and Peter K. Dorhout*[,†]

Department of Chemistry and Department of Physics, Colorado State University, Fort Collins, Colorado 80523, and Chemistry Division, Los Alamos National Laboratory, Los Alamos, New Mexico 87545

Received December 22, 2000

Six new actinide metal thiophosphates have been synthesized by the reactive flux method and characterized by single-crystal X-ray diffraction: $Cs_8U_5(P_3S_{10})_2(PS_4)_6$ (**I**), $K_{10}Th_3(P_2S_7)_4(PS_4)_2$ (**II**), $K_5U(PS_4)_3$ (**III**), $K_5Th(PS_4)_3$ (**IV**), $Rb_5Th(PS_4)_3$ (**V**), and $Cs_5Th(PS_4)_3$ (**VI**). Compound **I** crystallizes in the monoclinic space group $P2_1/c$ with $a = 33.2897(1)$ Å, $b = 14.9295(1)$ Å, $c = 17.3528(2)$ Å, $\beta = 115.478(1)°$, $Z = 8$. Compound **II** crystallizes in the monoclinic space group $C2/c$ with $a = 32.8085(6)$ Å, $b = 9.0482(2)$ Å, $c = 27.2972(3)$ Å, $\beta = 125.720(1)°$, $Z = 8$. Compound **III** crystallizes in the monoclinic space group $P2_1/c$ with $a = 14.6132(1)$ Å, $b = 17.0884(2)$ Å, $c = 9.7082(2)$ Å, $\beta = 108.63(1)°$, $Z = 4$. Compound **IV** crystallizes in the monoclinic space group $P2_1/n$ with $a = 9.7436(1)$ Å, $b = 11.3894(2)$ Å, $c = 20.0163(3)$ Å, $\beta = 90.041(1)°$, $Z = 4$, as a pseudo-merohedrally twinned cell. Compound **V** crystallizes in the monoclinic space group $P2_1/c$ with $a = 13.197(4)$ Å, $b = 9.997(4)$ Å, $c = 18.189(7)$ Å, $\beta = 100.77(1)°$, $Z = 4$. Compound **VI** crystallizes in the monoclinic space group $P2_1/c$ with $a = 13.5624(1)$ Å, $b = 10.3007(1)$ Å, $c = 18.6738(1)$ Å, $\beta = 100.670(1)°$, $Z = 4$. Optical band-gap measurements by diffuse reflectance show that compounds **I** and **III** contain tetravalent uranium as part of an extended electronic system. Thorium-containing compounds are large-gap materials. Raman spectroscopy on single crystals displays the vibrational characteristics expected for $[PS_4]^{3-}$, $[P_2S_7]^{4-}$, and the new $[P_3S_{10}]^{5-}$ building blocks. This new thiophosphate building block has not been observed except in the structure of the uranium-containing compound $Cs_8U_5(P_3S_{10})_2(PS_4)_6$.

Introduction

The use of molten alkali metal polychalcogenide fluxes has had a profound impact on the synthesis of complex ternary, quaternary, and quinary chalcogenide compounds.[1−3] This method has been used to synthesize numerous quaternary rare earth and actinide chalcophosphate compounds.[4−12] Quaternary f-block chalcophosphate compounds such as $K_3CeP_2S_8$, $A_3(RE)P_2Se_8$, and $A_2(RE)P_2Se_7$ (A = Rb, Cs; RE = Ce, Gd) have been synthesized using this method.[3,9,10,13−17] Recently, several new actinide compounds have been synthesized using molten alkali metal polychalcogenide fluxes including $K_2UP_3Se_9$ and $Rb_4U_4P_4Se_{26}$, and their Th analogues, and $Cs_4Th_2P_5Se_{17}$.[7,11,18−21] We report herein the synthesis and characterization of the first quaternary thorium and uranium *thiophosphate* compounds: $Cs_8U_5(P_3S_{10})_2(PS_4)_6$ (**I**), $K_{10}Th_3(P_2S_7)_4(PS_4)_2$ (**II**), $K_5U(PS_4)_3$ (**III**), $K_5Th(PS_4)_3$ (**IV**), $Rb_5Th(PS_4)_3$ (**V**), and $Cs_5Th(PS_4)_3$ (**VI**). These six new compounds exhibit structures ranging from three-dimensional extended networks to isolated dimers. The actinide atoms in these structures are linked together through thiophosphate ligands. The combination of the actinide elements and

* To whom correspondence should be addressed. Telephone: 970-491-0624. E-mail: pkd@LAMAR.colostate.edu.
† Department of Chemistry, Colorado State University.
‡ Department of Physics, Colorado State University.
# Los Alamos National Laboratory.

(1) Chondroudis, K.; McCarthy, T. J.; Kanatzidis, M. G. *Inorg. Chem.* **1996**, *35*, 840−844.
(2) Chung, D. Y.; Iordanidis, L.; Choi, K. S.; Kanatzidis, M. G. *Bull. Kor. Chem. Soc.* **1998**, *19*, 1283−1293.
(3) Chondroudis, K.; Kanatzidis, M. G. *Inorg. Chem.* **1998**, *37*, 3792.
(4) Chen, J. H.; Dorhout, P. K. *Inorg. Chem.* **1995**, *34*, 5705−5706.
(5) Chen, J. H.; Dorhout, P. K.; Ostenson, J. E. *Inorg. Chem.* **1996**, *35*, 5627−5633.
(6) Orgzall, I.; Lorenz, B.; Dorhout, P. K.; Van Calcar, P. M.; Brister, K.; Weishaupt, K.; Hochheimer, H. D. *J. Phys. Chem. Solids* **2000**, *61*, 123−124.
(7) Briggs Piccoli, P. M.; Abney, K. D.; Schoonover, J. R.; Dorhout, P. K. *Inorg. Chem.* **2000**, *39*, 2970−2976.
(8) Hess, R. F.; Abney, K. D.; Dorhout, P. K. In preparation.
(9) Evenson, C. R.; Dorhout, P. K. *Inorg. Chem.*, in press.
(10) Evenson, C. R.; Dorhout, P. K. *Inorg. Chem.*, in press.
(11) Briggs-Piccoli, P. M.; Abney, K. D.; Schoonover, J. D.; Dorhout, P. K. *Inorg. Chem.*, in press.
(12) Hess, R. F.; Abney, K. D.; Dorhout, P. K. *J. Am. Chem. Soc.*, in press.
(13) Gauthier, G.; Jobic, S.; Brec, R.; Rouxel, J. *Inorg. Chem.* **1998**, *37*, 2332−2333.
(14) Chondroudis, K.; Kanatzidis, M. G. *Inorg. Chem. Commun.* **1998**, *1*, 55−57.
(15) Chondroudis, K.; Kanatzidis, M. G. *Inorg. Chem.* **1998**, *37*, 3792−3797.
(16) Aitken, J. A.; Chondroudis, K.; Young, V. G. J.; Kanatzidis, M. G. *Inorg. Chem.* **2000**, *39*, 1525−1533.
(17) Gauthier, G.; Jobic, S.; Danaire, V.; Brec, R.; Evain, M. *Acta Crystallogr. C* **2000**, *56*, 117.
(18) Chondroudis, K.; Kanatzidis, M. G. *C. R. Acad. Sci. Paris* **1996**, *322*, 887−894.
(19) Chondroudis, K.; Kanatzidis, M. G. *J. Am. Chem. Soc.* **1997**, *119*, 2574−2575.
(20) Sutorik, A. C.; Kanatzidis, M. G. *Chem. Mater.* **1997**, *9*, 387−398.
(21) Sutorik, A. C.; Patschke, R.; Schindler, J.; Kannewurf, C. R.; Kanatzidis, M. G. *Chem. Eur. J.* **2000**, *6*, 1601−1607.

10.1021/ic0014437 CCC: $20.00
Published on Web 05/09/2001

Table 1. Crystallographic Data for Compounds **I**−**VI**

	I	II	III	IV	V	VI
empirical formula	$Cs_4U_{2.5}P_6S_{22}$	$K_5Th_{1.5}P_5S_{18}$	$K_5UP_3S_{12}$	$K_5ThP_3S_{12}$	$Rb_5ThP_3S_{12}$	$Cs_5ThP_3S_{12}$
fw	2017.85	1275.49	911.16	905.17	1137.02	1374.22
a, Å	33.2897(1)	32.8085(6)	14.6132(1)	9.7436(1)	13.197(4)	13.5624(1)
b, Å	14.9295(1)	9.0482(2)	17.0884(2)	11.3894(2)	9.997(4)	10.3007(1)
c, Å	17.3528(2)	27.2972(3)	9.7082(1)	20.0163(3)	18.189(7)	18.6738(1)
β, deg	115.478(1)	125.720(1)	108.63(1)	90.041(1)	100.77(1)	100.670(1)
V, Å^3	7785.6(1)	6579.0(2)	2297.31(4)	2221.28(6)	2357(2)	2563.66(3)
Z	8	8	4	4	4	4
λ(Mo Kα),Å	0.71073	0.71073	0.71073	0.71073	0.71073	0.71073
space group	$P2_1/c$ (14)	$C2/c$ (15)	$P2_1/c$ (14)	$P2_1/n$ (14)	$P2_1/c$ (14)	$P2_1/c$ (14)
temp, K	163(2)	163(2)	163(2)	163(2)	163(2)	163(2)
ρ_{calc}, g/cm^3	3.443	2.575	2.634	2.707	3.204	3.560
μ, mm^{-1}	15.50	8.80	9.26	8.98	17.84	13.97
R1, %[a]	0.0590	0.0346	0.0376	0.0363	0.0501	0.0452
wR2, %[a]	0.1156	0.0714	0.0744	0.0780	0.1111	0.1182

[a] $R1 = \sum(|F_o| - |F_c|)/\sum|F_o|$. $wR2 = [\sum[w(F_o^2 - F_c^2)^2]/\sum[w(F_o^2)^2]]^{1/2}$.

the thiophosphate flux has produced many interesting ligands all based on PS_4 tetrahedral building blocks. These ligands include $[PS_4]^{3-}$, $[P_2S_7]^{4-}$, and the previously unobserved $[P_3S_{10}]^{5-}$. Raman vibrational analysis, diffuse reflectance, and thermal analysis data are presented and discussed in the context of these new structures.

Experimental Section

General Synthesis. Red phosphorus powder (99.9%) was obtained from Cerac. Selenium shot (99.999%) was purchased from Johnson Matthey. ^{232}Th ribbon was obtained from Los Alamos National Laboratory. ^{238}U turnings (99.7%) were obtained from Cerac. A_2S_2 and A_2S_5 (A = K, Rb, Cs) were prepared from a stoichiometric ratio of the elements in liquid ammonia as described elsewhere.[22] *N*,*N*-dimethylformamide (DMF) was obtained from Aldrich and used without further purification. Initial searches for phases in these chemical systems were performed using stoichiometric compositions that resembled known lanthanide phases.[10] Reactions were optimized to produce high yields of the products once they were identified. Ampules for the reactions were all fused-silica tubes with a 4 mm inner diameter and a 6 mm outer diameter. All reagents were stored and manipulated in a helium filled glovebox. *Warning: ^{232}Th and ^{238}U are radioactive elements with half-lives of 1.41 × 10^{10} years and 4.47 × 10^9 years, respectively. Although their own activity is low, the inevitable daughter products of decay can render samples highly radioactive over time (γ).*

Synthesis of $Cs_8U_5(P_3S_{10})_2(PS_4)_6$, I. $Cs_8U_5(P_3S_{10})_2(PS_4)_6$ was synthesized from a mixture of 0.0248 g (0.10 mmol) of U, 0.0129 g (0.43 mmol) of P, 0.0251 g (0.78 mmol) of S, and 0.0666 g (0.16 mmol) of Cs_2S_5. The mixture was loaded into a fused silica ampule and sealed under vacuum. The ampule was then heated to 750 °C over 16 h and held there for 100 hours. The ampule was cooled to ambient temperature at a rate of 4 °C per hour. Excess flux was removed by washing with DMF. Amber rods were then isolated by filtration and selected crystals were hand-picked for analysis.

Synthesis of $K_{10}Th_3(P_2S_7)_4(PS_4)_2$, II. $K_{10}Th_3(P_2S_7)_4(PS_4)_2$ was synthesized from a mixture of 0.084 g (0.36 mmol) of Th, 0.0379 g (1.22 mmol) of P, 0.0447 g (1.39 mmol) of S, and 0.1805 g (0.760 mmol) of K_2S_5. The mixture was loaded into a fused silica ampule and sealed under vacuum. The ampule was then heated to 500 °C over 16 h and held there for 288 h. The ampule was cooled to ambient temperature at a rate of 3 °C/h. Excess flux was removed by washing with DMF. Clear, colorless rods were then isolated by filtration and selected crystals were hand-picked for analysis.

Synthesis of $K_5U(PS_4)_3$, III. $K_5U(PS_4)_3$ was synthesized from a mixture of 0.1041 g (0.44 mmol) of U, 0.0305 g (1.00 mmol) of P, 0.1713 g (5.3 mmol) of S, and 0.0994 g (0.700 mmol) of K_2S_2. The mixture was loaded into a fused silica ampule and sealed under vacuum. The ampule was then heated to 500 °C over 16 h and held there for 288 h. The ampule was cooled to ambient temperature at a rate of 3 °C per hour. Excess flux was removed by washing with DMF. Amber plates were then isolated by filtration and selected crystals were hand-picked for analysis.

Synthesis of $K_5Th(PS_4)_3$, IV. $K_5Th(PS_4)_3$ was synthesized from a mixture of 0.0626 g (0.27 mmol) of Th, 0.0252 g (0.81 mmol) of P, 0.0846 g (2.64 mmol) of S, and 0.0812 g (0.57 mmol) of K_2S_2. The mixture was loaded into a fused silica ampule and sealed under vacuum. The ampule was then heated to 500 °C over 16 h and held there for 288 h. The ampule was cooled to ambient temperature at a rate of 3 °C/h. Excess flux was removed by washing with DMF. Colorless irregular-shaped crystals were then isolated by filtration and selected crystals were hand-picked for analysis.

Synthesis of $Rb_5Th(PS_4)_3$, V. $Rb_5Th(PS_4)_3$ was synthesized from a mixture of 0.0779 g (0.36 mmol) of Th, 0.0356 g (1.17 mmol) of P, 0.1047 g (3.27 mmol) of S, and 0.1665 g (0.710 mmol) of Rb_2S_2. The mixture was loaded into a fused silica ampule and sealed under vacuum. The ampule was then heated to 500 °C over 16 h and held there for 288 h. The ampule was cooled to ambient temperature at a rate of 3 °C/h. Excess flux was removed by washing with DMF. Colorless rods were then isolated by filtration and selected crystals were hand-picked for analysis.

Synthesis of $Cs_5Th(PS_4)_3$, VI. $Cs_5Th(PS_4)_3$ was synthesized from a mixture of 0.0619 g (0.27 mmol) of Th, 0.0299 g (0.99 mmol) of P, 0.0320 g (1.00 mmol) of S, and 0.2320 g (0.54 mmol) of Cs_2S_5. The mixture was loaded into a fused silica ampule and sealed under vacuum. The ampule was then heated to 500 °C over 16 h and held there for 288 h. The ampule was cooled to ambient temperature at a rate of 3 °C per hour. Excess flux was removed by washing with DMF. Translucent, slightly green-tinted polyhedral cyrstals were then isolated by filtration and selected crystals were hand-picked for analysis.

Physical Characterization. Single-crystal X-ray diffraction was performed on a modified Siemens P4 four-circle diffractometer equipped with a SMART CCD system detector or a Siemens SMART CCD system using graphite-monochromated Mo Kα radiation. Elemental analysis confirming the stoichiometries of the compounds was obtained from Energy Dispersive Spectroscopy on a Philips 505 scanning electron microscope system equipped with a Kevex Analyst 8000 microanalyzer. UV−vis NIR spectra were recorded as diffuse reflectance spectra using a Cary 500 spectrometer equipped with praying-mantis reflectance focusing optics. The data were evaluated using the Kubelka−Munk relationship for diffuse reflectance data.[23] Only the data for the uranium compounds are shown. Raman spectra were recorded on a home-built optical bench using an Acton Research Spectra Pro-275 LN_2-cooled CCD detector (256 × 1024) using a controller model ST130 and a 50 mW HeNe laser line at 632.8.

Structure Determination. Crystals were selected from the reaction mixtures and mounted in grease and placed directly into the cold stream of the diffractometer on a glass fiber with the long axis of the crystals oriented roughly parallel to the length of the fiber. Cell constants for

(22) Liao, J.-H.; Kanatzidis, M. G. *Inorg. Chem.* **1992**, *31*, 431.

(23) Wilkinson, F.; Kelly, G. *Diffuse Reflectance Flash Photolysis*; CRC Press: Boca Raton, FL, 1989; Vol. 1.

Table 2. Fractional Atomic Coordinates and Equivalent Isotropic Displacement Parameters ($Å^2 \times 10^3$)[a] for $Cs_8U_5(P_3S_{10})_2(PS_4)_6$, **I**

	x	*y*	*z*	U(eq)
U(1)	0.0000	0.4182(1)	0.2500	12(1)
U(2)	0.0647(1)	0.1648(1)	0.3708(1)	11(1)
U(3)	−0.1585(1)	−0.2452(1)	0.1448(1)	12(1)
P(1)	0.1097(1)	−0.0399(3)	0.3649(3)	12(1)
P(2)	−0.0840(1)	−0.4267(3)	0.1907(2)	14(1)
P(3)	0.0459(1)	0.2487(3)	0.1568(2)	12(1)
P(4)	0.2494(1)	0.2396(3)	0.3284(3)	17(1)
P(5)	0.1369(1)	0.2172(3)	0.5834(2)	12(1)
P(6)	−0.2330(1)	−0.2944(3)	−0.1169(2)	13(1)
S(1)	0.0777(1)	0.3107(3)	0.2744(2)	13(1)
S(2)	0.0390(1)	0.5424(3)	0.1869(2)	18(1)
S(3)	0.0723(1)	0.4886(3)	0.3891(2)	18(1)
S(4)	0.0160(1)	0.3111(3)	0.4026(2)	13(1)
S(5)	0.0944(1)	0.1103(3)	0.5404(2)	15(1)
S(6)	0.0297(1)	0.1229(3)	0.1854(2)	15(1)
S(7)	0.1269(1)	0.2925(3)	0.4795(2)	16(1)
S(8)	0.1391(1)	0.0840(3)	0.3756(2)	16(1)
S(9)	0.0478(1)	−0.0183(3)	0.3597(3)	16(1)
S(10)	−0.1291(1)	−0.2912(3)	0.3261(2)	15(1)
S(11)	−0.2425(1)	−0.3245(3)	0.1034(3)	18(1)
S(12)	−0.0743(1)	−0.2966(3)	0.1668(3)	17(1)
S(13)	−0.1467(2)	−0.1206(3)	0.0353(2)	19(1)
S(14)	−0.1058(1)	−0.1015(3)	0.2429(2)	13(1)
S(15)	−0.1786(1)	−0.3390(3)	−0.0164(2)	19(1)
S(16)	−0.2159(1)	−0.1179(3)	0.1580(3)	17(1)
S(17)	−0.1475(1)	−0.4350(3)	0.1762(3)	17(1)
S(18)	0.0800(1)	−0.2491(3)	0.5887(2)	18(1)
S(19)	0.2002(1)	−0.1562(3)	0.1281(3)	16(1)
S(20)	0.2719(2)	0.1201(3)	0.3225(3)	22(1)
S(21)	0.2049(1)	0.2909(3)	0.2059(2)	16(1)
S(22)	0.2901(2)	−0.2449(3)	0.1152(3)	23(1)
Cs(1)	−0.0126(1)	−0.2209(1)	0.3882(1)	23(1)
Cs(2)	0.1574(1)	0.0680(1)	0.1819(1)	23(1)
Cs(3)	0.3743(1)	0.0193(1)	−0.1161(1)	26(1)
Cs(4)	0.2574(1)	−0.0446(1)	0.0054(1)	25(1)

[a] U(eq) is defined as one-third of the trace of the orthogonalized U_{ij} tensor.

Table 3. Selected Bond Distances (Å) for $Cs_8U_5(P_3S_{10})_2(PS_4)_6$, **I**

U(1)−S(2)	2.747(4)	P(1)−S(13)	2.032(6)
U(1)−S(3)	2.780(4)	P(1)−S(14)	2.038(6)
U(1)−S(1)	2.915(4)	P(1)−S(9)	2.048(6)
U(1)−S(4)	2.939(4)	P(1)−S(8)	2.063(6)
U(2)−S(8)	2.725(4)	P(2)−S(3)	2.033(6)
U(2)−S(9)	2.781(4)	P(2)−S(2)	2.058(6)
U(2)−S(5)	2.792(4)	P(2)−S(17)	2.022(6)
U(2)−S(7)	2.849(4)	P(2)−S(12)	2.041(6)
U(2)−S(1)	2.891(4)	P(3)−S(18)	1.961(6)
U(2)−S(4)	2.910(4)	P(3)−S(4)	2.084(6)
U(2)−S(6)	2.928(4)	P(3)−S(1)	2.069(6)
U(2)−S(6)	2.980(4)	P(3)−S(6)	2.073(6)
U(3)−S(12)	2.772(4)	P(4)−S(20)	1.954(6)
U(3)−S(16)	2.773(4)	P(4)−S(22)	1.961(6)
U(3)−S(13)	2.804(4)	P(4)−S(21)	2.142(6)
U(3)−S(11)	2.829(4)	P(4)−S(19)	2.171(6)
U(3)−S(14)	2.831(4)		
U(3)−S(17)	2.880(4)		
U(3)−S(15)	2.937(4)		
U(3)−S(10)	2.946(4)		

all structures were initially calculated from reflections taken from approximately 30 frames of reflections. Final cell constants were calculated from all reflections observed in the actual data collection. Table 1 summarizes the crystal structure parameters for compounds **I**−**VI**. For each structure, the data were processed and corrected for absorption using SADABS.[24] The structures were solved by direct methods allowing the unambiguous space group assignments and refined in full-matrix least-squares using the program SHELXTL[25] under the XSHELL package of programs.[26] For nearly every case, the final cycle of refinement included all anisotropic displacement parameters. Secondary extinction coefficients were applied to the final refinements. Additional experimental details are given in the Supporting Information. Specific refinement issues related to each structure are explained in the Results and Discussion section.

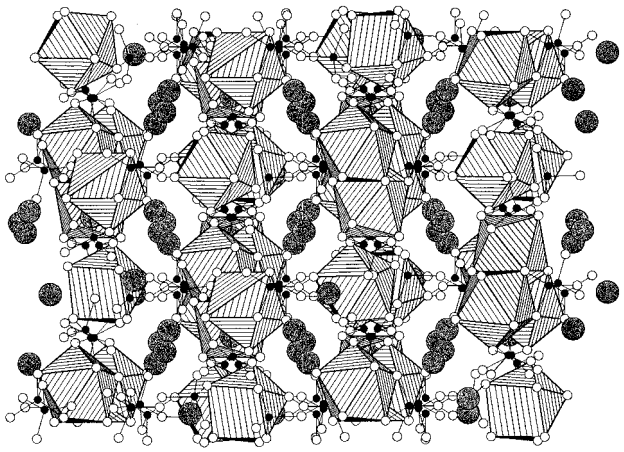

Figure 1. $Cs_8U_5(P_3S_{10})_2(PS_4)_6$, **I**, as viewed down [−10−1]. Polyhedra are US_8, cesium atoms are gray, phosphorus atoms are filled, and sulfur atoms are open circles.

Results and Discussion

$Cs_8U_5(P_3S_{10})_2(PS_4)_6$, I. The compound was isolated from the flux of the reaction by dissolution of the flux in DMF. Amber rodlike crystals were isolated by filtration and by hand sorting from undissolved flux. Table 1 lists specifics about the data collection and refinement. For the 19 869 reflections collected, the space group $P2_1/c$ was selected ($R_{int} = 0.097$) based on systematic absences. After solution and refinement and application of a secondary extinction coefficient, the largest unassigned peaks in the electron density map were 2.73 e/Å^3. Table 2 lists the atomic coordinates and Table 3 lists relevant bond distances.

Figure 1 shows a polyhedral view of the structure down the [−10−1] axis. This compound has a three-dimensional network structure built up of US_8 polyhedra and two different types of thiophosphate ligands, $[PS_4]^{3-}$ and the previously unknown $[P_3S_{10}]^{5-}$, a unit comprising three corner-sharing PS_4 tetrahedra. Three crystallographically distinct uranium atoms are found in the structure as US_8 bicapped trigonal prisms with an average U−S bond distance of 2.852 Å, distances comparable to uranium sulfide binary compounds. From Figure 1, one can see that the structure comprises layers bridged by thiophosphate groups. A view of one such layer is seen in Figure 2. In this view, one can easily distinguish the two types of thiophosphate polyhedra, $[PS_4]$ and $[P_3S_{10}]$. It is also possible to recognize that the uranium atoms form trimeric units (U1 and two U2) and isolated atoms (U3). Figure 3 shows a thermal ellipsoid plot of the trimeric unit. In this trimer of U(1) and two U(2) atoms, one finds four sulfur atoms on each metal that are shared with the neighboring U atom. This edge sharing among the U(1) and U(2) polyhedra forms a trimer unit where two $[PS_4]^{3-}$ tetrahedra cap the top and bottom of the trimer. The fourth S atom of the $[PS_4]^{3-}$ tetrahedron is a terminal atom, coordinating only with Cs^+ countercations. The cavity formed inside the trimer has the approximate dimensions: 4.85 Å × 4.83 Å × 5.32 Å and the closest U···U contact is 4.41 Å.

(24) Sheldrick, G. M. *SADABS*; University of Göttingen: Göttingen, Germany, 1997.

(25) Sheldrick, G. M. *SHELXTL*, version 5.; Siemens Analytical X-ray Instruments, Inc.: Madison, WI, 1997.

(26) Sheldrick, G. M. *XSHELL*; Siemens Analytical X-ray Instruments, Inc.: Madison, WI, 1999.

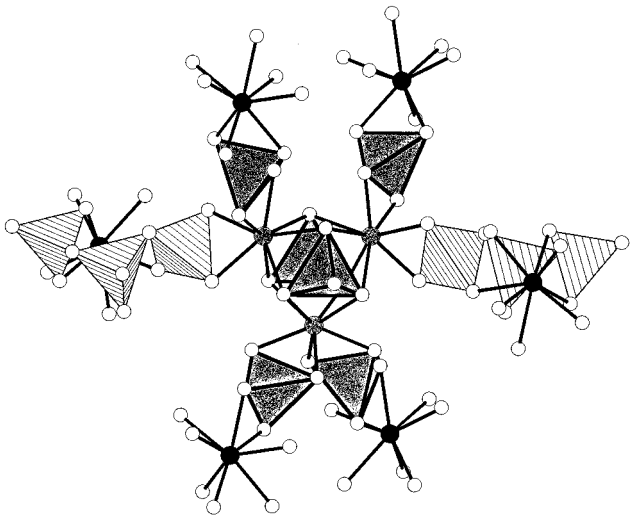

Figure 2. View of one layer in $Cs_8U_5(P_3S_{10})_2(PS_4)_6$, **I**, along [10−1] showing a U(1) and U(2) trimer (gray atoms) linked to six filled U(3) atoms by the $P_3S_{10}^{5-}$ units (striped tetrahedra). The PS_4^{3-} tetrahedra are shaded dark gray.

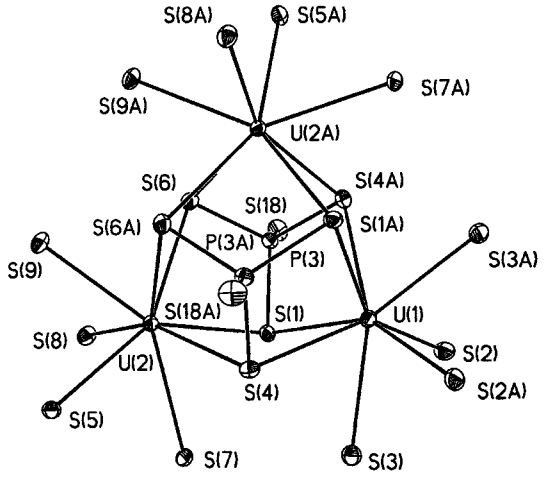

Figure 3. Thermal ellipsoid plot (50%) of the uranium trimer in $Cs_8U_5(P_3S_{10})_2(PS_4)_6$, **I**.

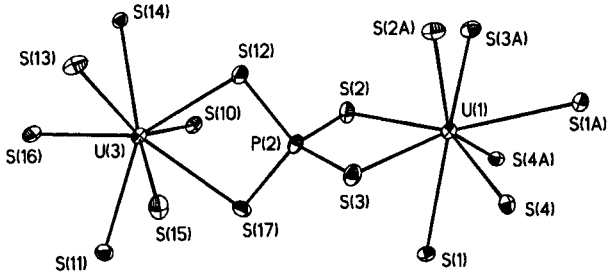

Figure 4. Thermal ellipsoid plot (50%) of the U(1)U(3) unit in $Cs_8U_5(P_3S_{10})_2(PS_4)_6$, **I**, showing the PS_4 link.

This trimer is the fundamental building block in this structure. Each individual trimer is linked to six U(3) polyhedra, two to U(1) and two to each U(2) polyhedra. It is through these U(3) polyhedra that the trimers are linked together to form a layer in the *ab* plane. The U(3) polyhedra are connected to the U(1) and U(2) polyhedra through two different thiophosphate tetrahedra, $[P(1)S_4]^{3-}$ and $[P(2)S_4]^{3-}$, seen in Figure 4. The U(3) polyhedra are also linked to each other via one end of the previously unknown $[P_3S_{10}]^{5-}$ ligand, as seen in the thermal ellipsoid plot, Figure 5. The $[P_3S_{10}]^{5-}$ unit effectively "chelates" one face of a U(3) atom while bridging U(2) and U(3) atoms

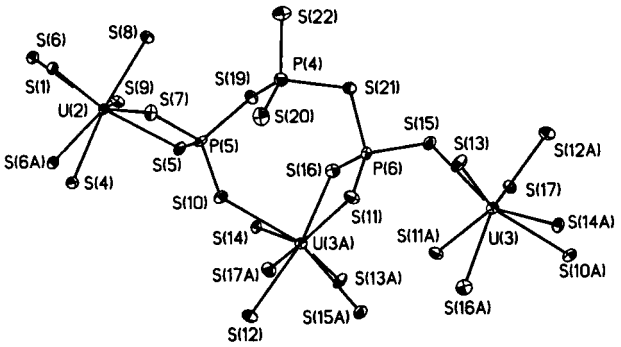

Figure 5. Thermal ellipsoid plot (50%) of the linkage to the new $[P_3S_{10}]^{5-}$ by three uranium atoms in $Cs_8U_5(P_3S_{10})_2(PS_4)_6$, **I**.

and establishing connectivity along the *a* direction. There is sufficient twisting in the $[P_3S_{10}]^{5-}$ that it no longer resembles $^3/_4$ of the $[P_4S_{12}]^{4-}$ ring that has been observed previously[27] or the $[P_4S_{10}]^{4-}$ cyclohexane-type thiophosphate.[28] The P(1) and P(2) tetrahedra both link to two U(3) polyhedra by sharing two of the thiophosphate-group edges. The individual layers are connected together along the *c* direction through $[P_3S_{10}]^{5-}$ ligands.

This connectivity creates tunnels that propagate through the structure. Tunnels exist along three different unit cell directions. One tunnel can be seen when the structure is viewed down the [101] direction and has the dimensions 5.9 Å × 18.8 Å. Two other tunnels can be seen when the structure is viewed down the [001] and [100] directions. Their respective dimensions are 8.7 Å × 8.9 and 6.7 Å × 11.5 Å. Four distinct Cs^+ cations exist in the structure and reside inside the tunnels. The Cs^+ cations are all coordinated by sulfur atoms only. Cs(1), Cs(2), and Cs(4) are all nine coordinate, and Cs(3) is eight coordinate. All the elements in this structure are found in oxidation states consistent with their known chalcogenide chemistry: Cs^+, U^{4+}, P^{5+}, and S^{2-}.

$K_{10}Th_3(P_2S_7)_4(PS_4)_2$, II. This compound crystallized as colorless rods in the centered monoclinic space group C2/*c* (R_{int} = 0.044) based on systematic absences in the data; crystallographic details can be found in Table 1. Tables 4 and 5 list the atomic coordinates and the relevant bond distances. The structure was solved without complications, except for the need for a secondary extinction coefficient (5.5×10^{-5}), leaving peaks in the difference map of 1.7 e/Å^3.

This compound displays a two-dimensional layered structure containing two crystallographically distinct Th atoms. Th(1) and Th(2) are both coordinated to eight sulfur atoms in a distorted dodecahedral geometry. Figure 6 is a polyhedral view of the structure down the [010] direction, showing the layers in the (011) planes that comprise two corrugated, interpenetrating layers of thorium thiophosphates. Figure 7 shows thermal ellipsoid plots of the coordination around each thorium atom and the $[PS_4]^{3-}$ and $[P_2S_7]^{4-}$ units. The Th−S bond distances range from 2.844 to 2.924 Å with an average distance of 2.905 Å. These ThS_8 dodecahedra are linked together to form layers via the two distinct thiophosphate ligands. All of the sulfur atoms coordinated to Th(1) and Th(2) are sulfide, S^{2-}, and are linked to phosphorus in the thiophosphate ligands. Th(1) is coordinated by one $[PS_4]^{3-}$ and two $[P_2S_7]^{4-}$ ligands while Th(2) is coordinated by one $[PS_4]^{3-}$ and three $[P_2S_7]^{4-}$ ligands (for

(27) Fransisco, R. H. P.; Tepe, T.; Eckert, H. *J. Solid State Chem.* **1993**, *107*, 452−459.
(28) Chondroudis, K.; Kanatzidis, M. G. *Inorg. Chem.* **1998**, *37*, 2098−2099.

Table 4. Fractional Atomic Coordinates and Equivalent Isotropic Displacement Parameters ($Å^2 \times 10^3$)[a] for $K_{10}Th_3(P_2S_7)_4(PS_4)_2$, **II**

	x	*y*	*z*	U(eq)
Th(1)	0.0000	0.09651(1)	0.2500	13(1)
Th(2)	0.1366(1)	0.06960(1)	0.5557(1)	13(1)
K(1)	0.1836(1)	0.0460(2)	0.4264(1)	27(1)
K(2)	0.0718(1)	0.2228(2)	0.6005(1)	64(1)
K(3)	0.0281(1)	1.3851(2)	0.3734(1)	34(1)
K(4)	0.2733(1)	0.4315(2)	0.7363(1)	28(1)
K(5)	0.1478(1)	0.5546(2)	0.3369(1)	44(1)
P(1)	0.0717(1)	0.8057(2)	0.3999(1)	15(1)
P(2)	0.0977(1)	0.6242(2)	0.6522(1)	16(1)
P(3)	0.1838(1)	0.0637(2)	0.6089(1)	15(1)
P(4)	0.1825(1)	0.3743(2)	0.5294(1)	18(1)
P(5)	0.1009(1)	0.1405(2)	0.2533(1)	16(1)
S(1)	0.0410(1)	0.6939(2)	0.3201(1)	21(1)
S(2)	0.0495(1)	1.2435(2)	0.2608(1)	19(1)
S(3)	0.0598(1)	1.0252(2)	0.3776(1)	20(1)
S(4)	0.0909(1)	0.9172(2)	0.2559(1)	25(1)
S(5)	0.0399(1)	0.7345(2)	0.4413(1)	19(1)
S(6)	0.1465(1)	0.7591(2)	0.4586(1)	18(1)
S(7)	0.2260(1)	0.5350(2)	0.5918(1)	19(1)
S(8)	0.1138(1)	0.3927(2)	0.5132(1)	22(1)
S(9)	0.2276(1)	0.8777(2)	0.6370(1)	19(1)
S(10)	0.1696(1)	0.6377(2)	0.6782(1)	21(1)
S(11)	0.0526(1)	0.6136(2)	0.5603(1)	21(1)
S(12)	0.1113(1)	1.0003(2)	0.5463(1)	20(1)
S(13)	0.0759(1)	0.8403(2)	0.6619(1)	21(1)
S(14)	0.0838(1)	0.0690(2)	0.6918(1)	24(1)
S(15)	0.1876(1)	0.3800(2)	0.4602(1)	40(1)
S(16)	0.2129(1)	0.1602(2)	0.5638(1)	18(1)
S(17)	0.1899(1)	0.1946(2)	0.6714(1)	22(1)
S(18)	0.1696(1)	0.2172(2)	0.3116(1)	24(1)

[a] U(eq) is defined as one-third of the trace of the orthogonalized U_{ij} tensor.

Table 5. Selected Bond Distances (Å) for $K_{10}Th_3(P_2S_7)_4(PS_4)_2$, **II**

Th(1)−S(3)	2.879(1)	P(1)−S(5)	2.039(2)
Th(1)−S(1)	2.912(2)	P(1)−S(6)	2.044(2)
Th(1)−S(3)	2.879(1)	P(2)−S(10)	2.032(2)
Th(1)−S(1)	2.913(2)	P(2)−S(11)	2.039(2)
Th(1)−S(2)	2.918(2)	P(2)−S(13)	2.150(2)
Th(1)−S(2)	2.918(2)	P(2)−S(14)	1.982(2)
Th(1)−S(4)	2.924(2)	P(3)−S(9)	2.049(2)
Th(1)−S(4)	2.924(2)	P(3)−S(12)	2.040(2)
Th(2)−S(12)	2.844(2)	P(3)−S(16)	2.136(2)
Th(2)−S(7)	2.886(1)	P(3)−S(17)	1.988(2)
Th(2)−S(5)	2.893(1)	P(4)−S(7)	2.053(2)
Th(2)−S(10)	2.898(1)	P(4)−S(8)	2.033(2)
Th(2)−S(8)	2.903(2)	P(4)−S(15)	1.992(2)
Th(2)−S(6)	2.911(1)	P(4)−S(16)	2.129(2)
Th(2)−S(11)	2.926(1)	P(5)−S(13)	2.131(2)
Th(2)−S(9)	2.968(1)	P(5)−S(18)	1.977(2)
P(1)−S(1)	2.055(2)	P(5)−S(2)	2.037(2)
P(1)−S(3)	2.047(2)	P(5)−S(4)	2.055(2)

clarity, all the thiophosphates are not included in the thermal ellipsoid plot). The unique $[PS_4]^{3-}$ ligand consists of a phosphorus atom, P(1), surrounded by four sulfur atoms in a distorted tetrahedral geometry. The P(1)−S bond distances range from 2.044 to 2.055 Å with an average distance of 2.046 Å, consistent with typical thiophosphate bond distances. This thiophosphate ligand links the Th(1) and Th(2) polyhedra along *c* crystallographic direction by sharing one edge (S(3) and S(1)) with Th(1) and another edge (S(5) and S(6)) with Th(2), as shown in Figure 7. Two distinct $[P_2S_7]^{4-}$ units exist in this structure. Both ligands are composed of two PS_4 tetrahedra that corner-share one sulfur atom, S(16) or S(13) in Figure 7. One $[P_2S_7]^{4-}$ ligand contains P(2) and P(5) with S(13) as the bridging atom. This ligand edge-shares to both Th(1) and Th(2) polyhedra thus connecting them along the *c* crystallographic direction. Two of the sulfur atoms in this ligand, S(14) and S(18), are not

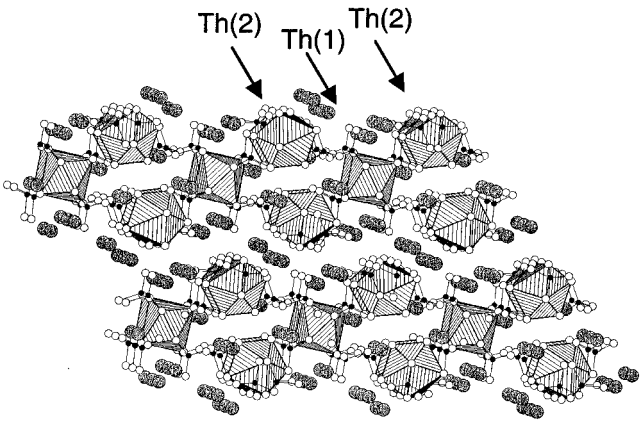

Figure 6. A polyhedral view of $K_{10}Th_3(P_2S_7)_4(PS_4)_2$, **II**, down [010]. Polyhedra are ThS_8, potassium atoms are gray spheres, phosphorus atoms are filled circles, and sulfur atoms are open circles. Stacking of Th(1) and Th(2) polyhedra is shown by the arrows.

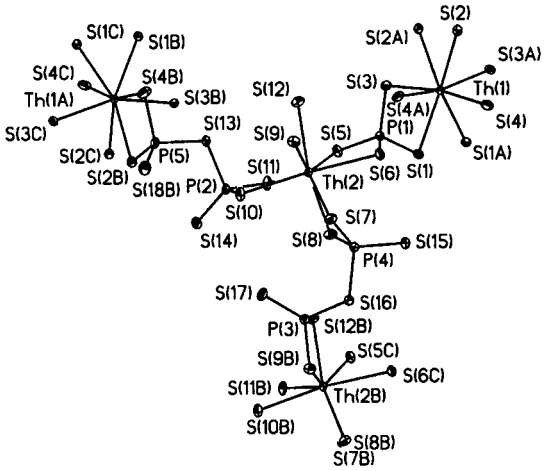

Figure 7. Thermal ellipsoid plot (50%) of the thorium thiophosphate network in $K_{10}Th_3(P_2S_7)_4(PS_4)_2$, **II**.

coordinated to thorium but are free terminal atoms that point into the interlayer space, interacting with potassium cations through long ionic interactions (3.1−3.9 Å). The other $[P_2S_7]^{4-}$ ligand contains P(3) and P(4) with S(16) as the bridging atom. This ligand links two different Th(2) polyhedra together along the *b* direction. Both S(15) and S(17) are terminal atoms that coordinate to interlayer potassium atoms. In the case of the two $[P_2S_7]^{4-}$ ligands, the phosphorus-to-corner shared sulfur atom distances are typically 0.1 Å longer than the average P−S distance. The phosphorus-to-terminal sulfur atom distances are significantly shorter (0.04 Å) than the average distance and are approximately equidistant between a phosphorus single and a double bond. The S−P−S bond angles are within the range expected for a PS_4 tetrahedron.

Each individual layer in this structure can be described as containing two rows of Th(2) polyhedra separated by one row of Th(1) polyhedra, where the rows run along the *b* direction in the layers, as shown in Figure 8. The Th(2) polyhedra are linked together along the c direction through Th(1) polyhedra. These polyhedra are linked via both $[PS_4]^{3-}$ and $[P_2S_7]^{4-}$ ligands. When a single layer is viewed down [101], as in Figure 8, it becomes apparent that the layer is built up of two intertwined chains with the composition Th(2)−$[P_2S_7]^{4-}$−Th(1)−$[PS_4]^{3-}$−Th(2). Connectivity between Th(1) and Th(2) along the *b* direction is established though $[P_2S_7]^{4-}$ only. These intertwined chains create channels that run along the *b* direction

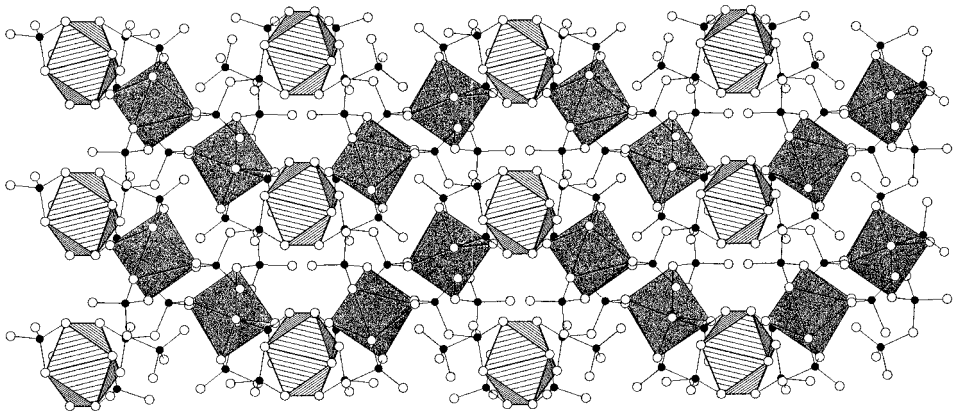

Figure 8. View down [101] of one layer of $K_{10}Th_3(P_2S_7)_4(PS_4)_2$, **II**. Th(1) are hatched polyhedra, Th(2) are shaded polyhedra. Potassium atoms have been removed for clarity.

Table 6. Fractional Atomic Coordinates and Equivalent Isotropic Displacement Parameters ($Å^2 \times 10^3$)[a] for $K_5U(PS_4)_3$, **III**

	x	*y*	*z*	U(eq)[a]	frac occup
U(1)	0.3337(1)	0.5008(1)	0.8902(1)	12(1)	
K(1)	0.2083(3)	0.8052(2)	0.6065(4)	37(1)	0.5
K(1A)	0.2306(2)	0.8070(2)	0.6748(4)	26(1)	0.5
K(2)	0.0143(1)	0.4704(1)	0.2153(2)	26(1)	
K(3)	−0.0765(1)	0.7037(1)	0.3429(2)	32(1)	
K(4)	0.3140(1)	0.4948(1)	0.4432(2)	33(1)	
K(5)	0.5530(1)	0.7008(1)	0.7185(2)	47(1)	
S(1)	0.4058(1)	0.6461(1)	0.0349(2)	18(1)	
S(2)	0.4783(1)	0.4759(1)	0.1717(2)	20(1)	
S(3)	0.3738(1)	0.3792(1)	0.7182(2)	28(1)	
S(4)	0.2790(1)	0.3512(1)	0.9537(2)	18(1)	
S(5)	0.2137(1)	0.5131(1)	0.0655(2)	17(1)	
S(6)	0.1585(1)	0.4860(1)	0.6577(2)	17(1)	
S(7)	0.3089(1)	0.6273(1)	0.6982(2)	21(1)	
S(8)	0.0820(1)	0.6721(1)	0.6840(2)	28(1)	
S(9)	0.1303(1)	0.6160(1)	0.3853(2)	28(1)	
S(10)	0.4361(2)	0.6275(1)	0.3892(2)	46(1)	
S(11)	0.2288(1)	0.3488(1)	0.2697(2)	27(1)	
S(12)	0.0509(1)	0.3663(1)	0.9574(2)	21(1)	
P(1)	0.1628(1)	0.6029(1)	0.6009(2)	15(1)	
P(2)	0.4835(1)	0.5943(1)	0.2274(2)	18(1)	
P(3)	0.1900(1)	0.3921(1)	0.0660(2)	16(1)	

[a] U(eq) is defined as one-third of the trace of the orthogonalized U_{ij} tensor.

Table 7. Selected Bond Distances (Å) for $K_5U(PS_4)_3$, **III**

U(1)−S(7)	2.802(2)	P(1)−S(6)	2.078(2)
U(1)−S(4)	2.805(1)	P(1)−S(7)	2.083(2)
U(1)−S(5)	2.814(2)	P(2)−S(10)	1.991(3)
U(1)−S(6)	2.832(1)	P(2)−S(10A)	2.032(2)
U(1)−S(3)	2.842(2)	P(2)−S(2)	2.052(2)
U(1)−S(2)	2.881(1)	P(2)−S(1)	2.089(2)
U(1)−S(1)	2.903(1)	P(3)−S(11)	2.015(2)
U(1)−S(2A)	3.021(2)	P(3)−S(12)	2.017(2)
P(1)−S(9)	2.005(2)	P(3)−S(4)	2.068(2)
P(1)−S(8)	2.012(2)	P(3)−S(5)	2.098(2)

within each layer. These channels have dimensions 13.667 Å × 4.358 Å. The closest Th···Th distance within the layers is 7.210 Å.

Five distinct K^+ cations exist in this structure, all of which are coordinated to S atoms. K(1) and K(4) are coordinated by seven S atoms, K(2) is coordinated by five S atoms, K(3) is coordinated by eight S atoms, and K(5) is coordinated by six S atoms. The average K−S distance is 3.371 Å. The potassium atoms K(1), K(4), and K(5) all lie between the layers, though they are not symmetrically situated with respect to the centers of the channels. The potassium atoms K(2) and K(3) both lie within the channels contained in the *bc* plane, described above.

Table 8. Fractional Atomic Coordinates and Equivalent IsotropicDisplacement Parameters ($Å^2 \times 10^3$)[a] for $K_5Th(PS_4)_3$, **IV**

	x	*y*	*z*	U(eq)[a]
Th(1)	0.1070(1)	0.6489(1)	0.0806(1)	10(1)
K(1)	0.1131(4)	0.6558(1)	−0.2574(1)	20(1)
K(2)	0.1814(2)	0.9057(2)	−0.0974(1)	29(1)
K(3)	−0.3595(2)	0.5902(2)	0.0834(1)	39(1)
K(4)	0.6706(3)	0.6062(2)	−0.2498(1)	32(1)
K(5)	0.3802(2)	0.1412(1)	0.0795(1)	20(1)
P(1)	0.3810(2)	0.8118(2)	0.0793(1)	13(1)
P(2)	−0.0930(3)	0.6718(1)	−0.0812(1)	12(1)
P(3)	0.4023(3)	0.8312(2)	−0.2623(1)	13(1)
S(1)	0.2638(2)	0.4343(2)	0.0801(2)	19(1)
S(2)	−0.0772(2)	0.4367(2)	0.0692(1)	14(1)
S(3)	−0.0949(4)	0.7732(2)	0.0026(1)	34(1)
S(4)	0.0737(2)	0.5672(2)	0.2197(1)	16(1)
S(5)	−0.0954(4)	0.7784(2)	0.1554(1)	27(1)
S(6)	0.2017(2)	0.9064(2)	0.0784(2)	24(1)
S(7)	0.3589(2)	0.7025(2)	−0.0018(1)	19(1)
S(8)	0.3577(2)	0.7027(2)	0.1603(1)	19(1)
S(9)	0.0582(2)	0.6000(2)	−0.4194(2)	18(1)
S(10)	−0.0942(3)	0.7732(2)	−0.1621(1)	19(1)
S(11)	0.2742(3)	0.4256(2)	−0.2383(1)	21(1)
S(12)	0.4167(3)	0.7358(2)	−0.1778(1)	19(1)

[a] U(eq) is defined as one-third of the trace of the orthogonalized U_{ij} tensor.

Table 9. Selected Bond Distances for $K_5Th(PS_4)_3$, **IV**

Th(1)−S(1)	2.882(2)	P(1)−S(8)	2.056(3)
Th(1)−S(5)	2.882(2)	P(1)−S(7)	2.058(3)
Th(1)−S(3)	2.883(3)	P(2)−S(10)	1.989(3)
Th(1)−S(4)	2.954(2)	P(2)−S(3)	2.036(3)
Th(1)−S(8)	2.980(2)	P(2)−S(1)	2.057(3)
Th(1)−S(2)	3.020(2)	P(2)−S(2)	2.082(3)
Th(1)−S(7)	3.021(2)	P(3)−S(12)	2.016(3)
Th(1)−S(6)	3.074(2)	P(3)−S(11)	2.027(4)
Th(1)−S(2A)	3.168(2)	P(3)−S(4)	2.063(4)
P(1)−S(9)	1.998(2)	P(3)−S(5)	2.068(3)
P(1)−S(6)	2.052(3)		

As there are no S−S bonds present in this structure, the oxidation states of the elements can be assigned as follows: K^+, Th^{4+}, P^{5+}, and S^{2-}. Thorium in the 4+ oxidation state is consistent with its known chalcophosphate chemistry.[7,11]

Differential thermal analysis data indicate that while the $K_{10}Th_3(P_2S_7)_4(PS_4)_2$ was prepared by heating to 500 °C in a flux, it decomposes at 391 °C under nitrogen. A large exothermic peak is found just before the decomposition peak that may indicate a phase change that is not reversible.

$K_5U(PS_4)_3$ (III), $K_5Th(PS_4)_3$ (IV), $Rb_5Th(PS_4)_3$ (V), and $Cs_5Th(PS_4)_3$ (VI). Compounds **III**−**VI** are nearly isostructural, consisting of dimers of actinide atoms linked through thiophos-

Table 10. Fractional Atomic Coordinates and Equivalent Isotropic Displacement Parameters ($Å^2 \times 10^3$)[a] for $Rb_5Th(PS_4)_3$, **V**

	x	*y*	*z*	U(eq)
Th(1)	0.1853(1)	0.1010(1)	0.0351(1)	8(1)
P(1)	0.2871(2)	0.3717(3)	−0.0193(2)	10(1)
P(2)	0.0326(2)	0.9086(3)	−0.1346(2)	10(1)
P(3)	0.6428(2)	0.1040(3)	−0.1800(2)	11(1)
S(1)	0.0422(2)	0.2557(3)	0.1020(2)	13(1)
S(2)	0.0289(2)	−0.0732(3)	0.0893(2)	14(1)
S(3)	0.1840(2)	−0.0956(3)	−0.0823(2)	18(1)
S(4)	0.2758(2)	0.0680(3)	0.1952(2)	14(1)
S(5)	0.3436(2)	−0.1036(3)	0.0645(2)	19(1)
S(6)	0.3573(2)	0.1989(3)	−0.0449(2)	15(1)
S(7)	0.1351(2)	0.3395(3)	−0.0666(2)	14(1)
S(8)	0.2933(2)	0.3541(3)	0.0943(1)	13(1)
S(9)	0.6574(2)	0.4525(3)	0.0475(2)	14(1)
S(10)	0.0238(2)	0.9044(3)	−0.2453(2)	17(1)
S(11)	0.7072(2)	0.2720(3)	−0.2128(2)	15(1)
S(12)	0.4932(2)	0.0927(3)	−0.2299(2)	16(1)
Rb(1)	0.5151(1)	0.3877(1)	−0.1281(1)	16(1)
Rb(2)	0.1527(1)	0.6118(1)	−0.1910(1)	16(1)
Rb(3)	0.2044(1)	0.1570(1)	−0.2221(1)	31(1)
Rb(4)	0.5296(1)	0.1768(1)	0.1240(1)	25(1)
Rb(5)	0.1407(1)	−0.3608(1)	0.0526(1)	23(1)

[a] U(eq) is defined as one-third of the trace of the orthogonalized U_{ij} tensor.

Table 11. Selected Bond Distances (Å) for $Rb_5Th(PS_4)_3$, **V**

Th(1)−S(1)	2.881(3)	P(1)−S(7)	2.055(4)
Th(1)−S(3)	2.899(3)	P(1)−S(8)	2.060(4)
Th(1)−S(5)	2.901(3)	P(2)−S(10)	1.995(4)
Th(1)−S(4)	2.953(3)	P(2)−S(3)	2.047(4)
Th(1)−S(8)	3.003(3)	P(2)−S(1)	2.061(4)
Th(1)−S(2)	3.004(3)	P(2)−S(2)	2.073(4)
Th(1)−S(7)	3.015(3)	P(3)−S(12)	2.017(4)
Th(1)−S(6)	3.076(3)	P(3)−S(11)	2.022(4)
Th(1)−S(2A)	3.285(3)	P(3)−S(4)	2.073(4)
P(1)−S(9)	2.008(4)	P(3)−S(5)	2.076(4)
P(1)−S(6)	2.055(4)		

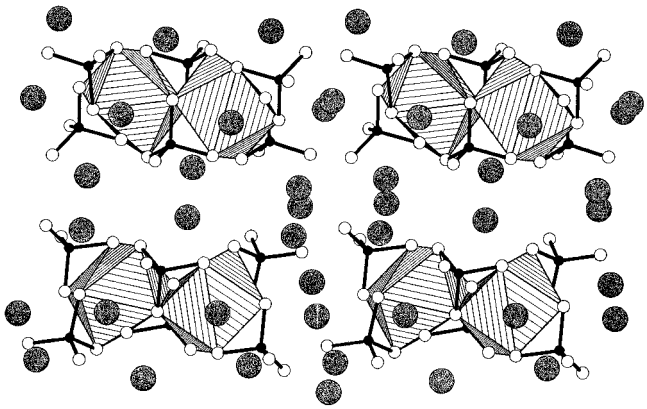

Figure 9. Polyhedral view of $K_5U(PS_4)_3$, **III**, down [00−1]. Potassium atoms are gray circles, phosphorus atoms are filled circles, and sulfur atoms are open circles.

phate bridges with significant differences in the packing arrangements of these dimers and the coordination of the thiophosphates within each dimer. Each compound (**III**−**VI**) crystallizes in a primitive monoclinic space group, as listed in Table 1. The atomic coordinates for **III**, **IV**, and **V** and relevant bond distances are listed in Tables 6−11, respectively.

$K_5U(PS_4)_3$ (III). This structure consists of discrete dimers of uranium polyhedra packed in the unit cell with potassium cations filling the voids between the dimers, as shown in the polyhedral representation in Figure 9. Packing problems associated with the larger $[U_2(PS_4)_6]^{10-}$ dimeric unit and relatively small potassium cations caused a disorder problem in the

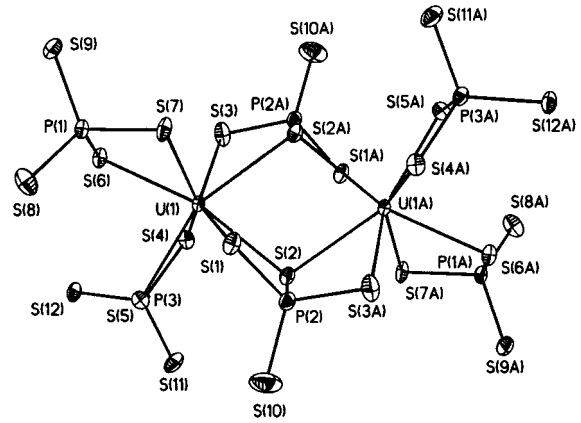

Figure 10. Thermal ellipsoid plot (50%) of the $[U_2(PS_4)_6]^{10-}$ dimer in $K_5U(PS_4)_3$, **III**.

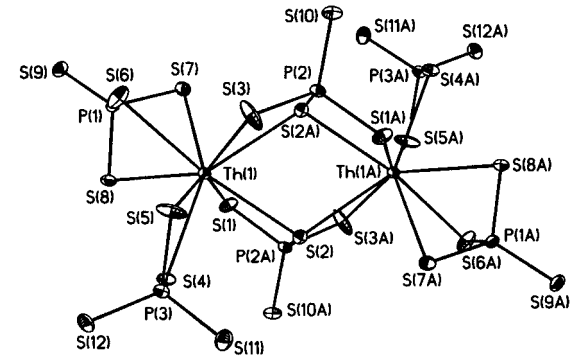

Figure 11. Thermal ellipsoid plot (50%) of the $[Th_2(PS_4)_6]^{10-}$ dimer in $K_5Th(PS_4)_3$, **IV**.

solution of the structure—K(1) and K(1A) are each modeled as 50% occupied and could not be modeled well with anisotropic thermal ellipsoids. The dimers are composed of two crystallographically identical uranium atoms that are linked together through sharing of two $[PS_4]^{3-}$ ligands across an inversion center. A thermal ellipsoid plot of the local coordination may be seen in Figure 10. The uranium atom is coordinated to eight sulfur atoms in a dodecahedral geometry. All eight sulfur atoms belong to face-capping or edge-bridging distinct $[PS_4]^{3-}$ ligands, each of which has a slightly distorted tetrahedral geometry. The tetrahedron centered on P(1) has two sulfur atoms (S(6) and S(7)) that are bound to one uranium atom in an edge-sharing arrangement with the two sulfur atoms (S(8) and S(9)) coordinated only to potassium cations. The P(2) tetrahedron and the U(1) polyhedron share a common edge of atoms S(2) and S(3) and the P(2) tetrahedron and the U(1A) polyhedron share a common edge of atoms S(1) and S(2). The fourth sulfur atom on P(2), S(10), is terminal, being coordinated only to potassium cations. Finally, the P(3) tetrahedron and the U(1) polyhedron also share a common edge of two sulfur atoms (S(4) and S(5)). The other two sulfur atoms on P(3), S(11) and S(12), are terminal. The bridging nature of the thiophosphates is not enough to bring the electron-poor uranium atoms within bonding distance, the closest U−U contact is 4.643(2) Å.

What will become significant later in the discussion of compounds **III**−**VI** are the bond distances across the dimer from An(1)−S(2A) and from S(2A)−An(1A), as well as the S(9)−P(1)−An(1) tilt angle of the $P(1)S_4$ tetrahedron. In **III**, the key U−S(2A) and S(2A)−U(1A) distances are 2.903(2) and 3.021(2) Å, respectively. The angle of tilt in the $P(1)S_4$ tetrahedron, S(9)−P(1)-U(1), is 139°, indicating that the triangular face comprising S(6), S(7), and S(8) is tilted away from the uranium

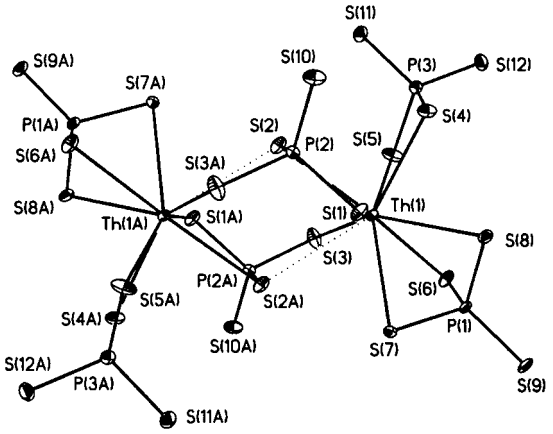

Figure 12. Thermal ellipsoid plot (50%) of the $[Th_2(PS_4)_6]^{10-}$ dimer in $Rb_5Th(PS_4)_3$, **V**. Dotted line indicates long Th−S interaction.

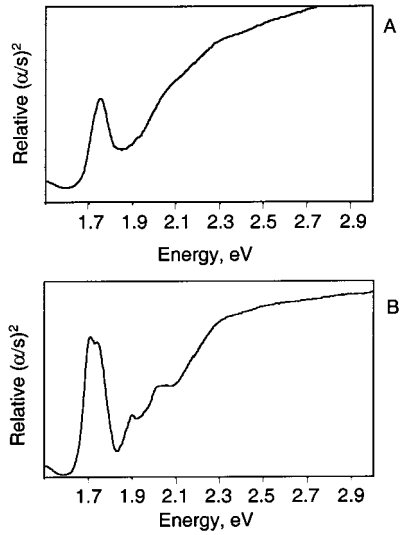

Figure 13. Diffuse reflectance spectra of (A) $Cs_8U_5(P_3S_{10})_2(PS_4)_6$, **I**, and (B) $K_5U(PS_4)_3$, **III**.

polyhedron and S(8) is not within bonding distance to U(1); the U(1)−S(8) contact distance is 4.625(2) Å.

Finally, all five K^+ cations are coordinated only to S atoms. K(1), K(2), and K(4) are eight coordinate while K(3) and K(5) are both nine coordinate. The K−S bond distances range from 3.170(4) Å to 3.960(4) Å with an average distance of 3.52 Å.

$K_5Th(PS_4)_3$, IV. The structure of **IV** is related to **III** in that it also consists of two actinide atoms, coordinated by thiophosphate ions, to form dimeric units in the monoclinic lattice. It was necessary to solve the structure of **IV** as a pseudomerohedrally twinned monoclinic unit cell, with the final twin component of the modeled lattice refining to a BASF value of 0.553(1).[29] Note the relationship of the 9.7 Å *c*-axis in **III** to the 9.7 Å *a*-axis in **IV**.

Figure 11 shows the thermal ellipsoid plot of the thorium dimer. The most striking contrasts between **III** and **IV** can be found in the P(1) thiophosphate ligands. In **IV**, thiophosphate $P(1)S_4$ caps a triangular face of the 9-coordinate thorium atoms; whereas in **III**, the same phosphate group is only edge-bridging. Now S(8) is located 3.074(2) Å from Th(1). The angle formed by S(9)−P(1)−Th(1) is 175°—a nearly linear arrangement, indicating that the triangular face formed by S(6), S(7), and

(29) BASF is part of the SHELXTL program, Siemens Analytical X-ray Systems, Inc.: Madison, WI, 1998.

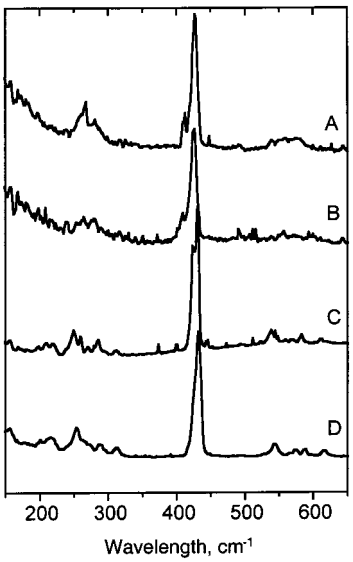

Figure 14. Raman spectra of (A) $Cs_8U_5(P_3S_{10})_2(PS_4)_6$, **I**, (B) $K_5U(PS_4)_3$, **III**, (C) $Rb_5Th(PS_4)_3$, **V**, and (D) $K_{10}Th_3(P_2S_7)_4(PS_4)_2$, **II**.

S(8) is nearly perpendicular to the S(9)−Th(1) line. Indeed, S(8) is within normal bonding distance to Th(1).

As in **III**, the dimer is bridged by two edges on the $P(2)S_4$ sharing across the gap, having S(2) on phosphate P(2) bridging to both Th(1) and Th(1A) through bonds 3.167(2) and 3.020(2) Å, thereby causing the two P(2) phosphates, related by the center of inversion, to act as η^2-type ligands on each thorium atom as we saw in **III**. It should be noted that the long bond distance has increased significantly from 3.021(2) Å to 3.167(2) Å between the actinide atoms and the bridging atom S(2). This coordination extension brings the two Th(IV) centers only to within 5.125(2) Å, a much longer An−An interaction than in **III**.

Finally, all five K^+ cations are coordinated only to S atoms. K(1), K(2), and K(4) are eight coordinate. K(3) and K(5) are both nine coordinate. The K−S bond distances range from 3.170 to 3.96 Å with an average distance of 3.52 Å.

The structural differences between **III** and **IV** may arise from arrangements in packing. Viewed along the common *a*-axis dimension, the two structures display significant differences. Both pack the dimers in layers, with interleaving potassium cations, but the packing arrangements are significantly different. In **III**, the dimers pack in parallel, tilted within one layer, with the alternating layer packing in the opposite direction. In **IV**, the packing resembles a herringbone arrangement within and between layers.

$Rb_5Th(PS_4)_3$ and $Cs_5Th(PS_4)_3$, V and VI. These two compounds are isostructural to each other and are related to the monoclinic cells of compounds **III** and **IV** by the unique axis of the monoclinic cells of **V** and **VI** being the 9.9−10 Å axis (the *c*-axis in **III** and the *a*-axis in **IV**). Only **V** will be shown for brevity; a thermal ellipsoid plot of **VI** is available in the Supporting Information. A thermal ellipsoid plot of **V** is shown in Figure 12. As found in **III** and **IV**, the compound consists of isolated dimers of actinides linked through thiophosphate ligands. In **V**, the $P(2)S_4$ unit bridges Th(1) and Th(1A) through sharing the S(2)S(1) edge with Th(1) but bonding to Th(1A) through only S(3A). The distance between S(2) and Th(1A) is a long 3.285(3) Å, as indicated by a dotted line in the figure. By contrast, the S(2)−Th(1) distance is 3.004(2) Å. The S(9)−P(1)-Th(1) tilt angle of the PS_4 tetrahedron is again nearly linear in **V**, at 174°, compared to the same angle in **IV**

Table 12. Raman Spectral Data of Selected Compounds (Vibrational Frequencies, cm^{-1}, and Relative Intensities)[a]

$Cs_8U_5P_{12}S_{44}$	$K_{10}Th_3P_{10}S_{36}$	$K_5UP_3S_{12}$	$Rb_5ThP_3S_{12}$	$CuHgPS_4$ ref 32	assignments PS_4 in T_d	$Ag_4P_2S_7$ ref 34	assignments P_2S_7 in C_{2v}
	215 m		210 w			203 m	ν_{20} (B_2)
265 m	254 m	260 w	254 m	236 m	ν_2 (E)	247 m	ν_9 (A_2)
300 w	289 m, 315 m	279 w	287 m	298 s	ν_4 (T_2)	300 m	ν_{13} (B_2)
425 vs	431 vs	424 s	430 vs	402 vs	ν_1 (A_1)	400 vs	ν_3 (A_1)
480 w						477 m	ν_{17} (B_2)
		500 w	490 vw	509 w	ν_3 (T_2)		
						516 m	ν_2 (A_1)
540 w	540 m	550 w	540 m	540 m	ν_3 (T_2)	555 m	ν_2 (A_1)
570 w	570 w	575 w	579 w	570 m	ν_3 (T_2)		
	590 w					590 w	ν_1 (A_1)
	615 w					602 w	ν_{12} (B_1)

[a] Assignments are from refs 32 and 34.

(175°). The dimer in **VI** has even more contrasting features with the Th(1)−S(2) and Th(1)−S(2A) distances being 2.990(3) and 3.429(3) Å, respectively. However, the tilt angle of the PS_4 tetrahedron, S(9)−P(1)-Th(1) is quite comparable at 175°. Packing of the dimers in **V** and **VI** are quite similar to the packing found in compound **IV**, with a herringbone-style packing arrangements in the layers. It is likely that the increased lengthening of the S(2)−Th(1) interactions is due to packing interactions related to the different alkali metal cations within the lattice. The tilting of the $P(1)S_4$ tetrahedra on the dimers may also be due to packing forces. For a direct comparison, however, it would be necessary to compare the alkali metal series A = K, Rb, Cs directly between the different actinide elements. However, to date, we have been unable to isolate $A_5U(PS_4)_3$, where A = Rb, Cs. Instead, either only compound **I** is found in the reactions or new phases, yet to be identified, are isolated.

Electronic Spectroscopy. Diffuse reflectance spectroscopy was used to analyze the electronic structure of the materials. Only the spectra for the two uranium compounds, **I** and **III**, are shown in Figure 13 for brevity. Band gap analysis using UV−vis NIR diffuse reflectance spectroscopy indicates that $K_{10}Th_3(P_2S_7)_4(PS_4)_2$, **II**, has a band gap energy of 3.3 eV and $K_5Th(PS_4)_3$, **IV**, has a band gap energy of 3.0 eV. These values are expected for colorless compounds. Based on the analysis of compounds **I** and **III**, the materials have a complex electronic structure dominated by the U(IV) electronic manifold. The classically ligand-to-metal charge-transfer peak seen in electronic spectra of aqueous U(IV) ions near 660 nm is observed in our compounds at around 730 nm (~1.7 eV).[30] Indeed, some fine structure is observed in the spectrum of **III**. The shift to lower energy is likely because the energy levels of the thiophosphate ligand are closer to the empty f-orbitals on uranium, indicating a more *covalent* bonding relationship with the thiophosphate than is observed in the ionic or dipolar relationships found in solution. Another general feature of the spectra is that they both show a broad rise in relative absorption beginning near 1.9 eV, consistent with the color of the materials and indicating some level of band structure to the electronic structure of the materials.

Raman Spectroscopy. Raman spectra were collected on hand-picked crystals of the compounds and are shown in Figure 14. The general features of the spectra comprise low-energy peaks indicative of the PS_4 tetrahedral units, spectra dominated by the symmetric stretch near 430 cm^{-1}. Specifically, peaks are recorded in Table 12 and assigned based on the pseudo-tetrahedral symmetry of the PS_4 units in all compounds and the P_2S_7 or P_3S_{10} units in compounds **I** and **II**.[31−34] These spectra are in relatively good agreement with the literature except for the shift to higher energy of the totally symmetric, high-intensity peak in all the spectra that can come about due to the relative binding of the thiophosphate to the actinide metal atoms. The main symmetric stretching mode of the PS_4 units is observed in each sample. Several other low energy peaks related to the tetrahedral stretching modes (four total) or pseudo-C_{2v} symmetry of the P_2S_7 unit found in $Ag_4P_2S_7$.[34]

Conclusions

In this paper, we have introduced six new thiophosphate actinide materials prepared using the thiophosphate high-temperature flux reaction on actinide metals. The compounds range in structural diversity from three-dimensional solids interconnected through the new $P_3S_{10}^{3-}$ ligand to a series of related dimers bridged by the PS_4^{3-} ligand and affected by packing forces. The new compounds have been studied by electronic spectroscopy (diffuse reflectance) and by Raman vibrational analysis. These methods confirm the electronic and structural diversity that comprise these six new compounds. Magnetic measurements, which were not performed on these compounds, are being considered. Recent forays into heavier actinides have demonstrated further unique materials comprising thiophosphate ligands: $KPuP_2S_7$ and $K_3PuP_2S_8$.[12] These actinide studies have demonstrated the unique differences between the chemistry of these heavier 5f elements and that of their lighter 4f lanthanide counterparts[9,10] illustrating the importance of the size and chemistry of the actinides.

Acknowledgment. This research was supported by DOE grant number DE-FG03-97ER14797 and the G. T. Seaborg Institute for Transctinium Science at Los Alamos National Laboratory. We also thank Dr. Harry Dewey of LANL for helpful discussions about electronic spectroscopy.

Supporting Information Available: Additional crystallographic details, tables of all bond distances and angles, anisotropic thermal parameters, and ORTEP figures. This material is available free of charge via the Internet at http://pubs.acs.org.

IC0014437

(30) Katz, J. J.; Seaborg, G. T.; Morss, L. R. *The Chemistry of the Actinide Elements*; Chapman and Hall: New York, 1986; Vol. 1, p 218.

(31) Carrillo-Cabrera, W.; Peters, K.; von Schnering, H. G.; Mentzel, F.; Brockner, W. *Z. Anorg. Allg. Chem.* **1995**, *621*, 557−561.

(32) Menzel, F.; Brockner, W.; Carrillo-Cabrera, W. *Heteroat. Chem.* **1993**, *4*, 393−398.

(33) Pätzmann, U.; Brockner, W.; Cyvin, B. N.; Cyvin, S. J. *J. Raman Spectrosc.* **1986**, *17*, 257−261.

(34) Mentzel, F.; Ohse, L.; Brockner, W. *Heteroat. Chem.* **1990**, *1*, 357−362.